



On the importance of multiphase photolysis of organic nitrates on their global atmospheric removal

Juan Miguel González-Sánchez^{1,2}, Nicolas Brun^{1,2}, Junteng Wu¹, Sylvain Ravier¹, Jean-Louis Clément², and Anne Monod¹

¹Aix Marseille Univ, CNRS, LCE, Marseille, France

²Aix Marseille Univ, CNRS, ICR, Marseille, France

Correspondence: Juan Miguel González-Sánchez (juangonzalez.sc@proton.me) and Anne Monod (anne.monod@univ-amu.fr)

Received: 10 January 2023 – Discussion started: 11 January 2023

Revised: 7 April 2023 – Accepted: 29 April 2023 – Published: 26 May 2023

Abstract. Organic nitrates (RONO_2) are secondary compounds, and their fate is related to the transport and removal of NO_x in the atmosphere. While previous research studies have focused on the reactivity of these molecules in the gas phase, their reactivity in condensed phases remains poorly explored despite their ubiquitous presence in submicron aerosols. This work investigated for the first time the aqueous-phase photolysis-rate constants and quantum yields of four RONO_2 (isopropyl nitrate, isobutyl nitrate, α -nitrooxyacetone, and 1-nitrooxy-2-propanol). Our results showed much lower photolysis-rate constants for these RONO_2 in the aqueous phase than in the gas phase. From alkyl nitrates to polyfunctional RONO_2 , no significant increase of their aqueous-phase photolysis-rate constants was observed, even for RONO_2 with conjugated carbonyl groups, in contrast with the corresponding gas-phase photolysis reactions. Using these new results, extrapolated to other alkyl and polyfunctional RONO_2 , in combination with estimates for the other atmospheric sinks (hydrolysis, gas-phase photolysis, aqueous- and gas-phase $\bullet\text{OH}$ oxidation, dry and wet deposition), multiphase atmospheric lifetimes were calculated for 45 atmospherically relevant RONO_2 along with the relative importance of each sink. Their lifetimes range from a few minutes to several hours depending on the RONO_2 chemical structure and its water solubility. In general, multiphase atmospheric lifetimes are lengthened when RONO_2 partition to the aqueous phase, especially for conjugated carbonyl nitrates for which lifetimes can increase by up to 100 %. Furthermore, our results show that aqueous-phase $\bullet\text{OH}$ oxidation is a major sink for water-soluble RONO_2 ($K_H > 10^5 \text{ M atm}^{-1}$) ranging from 50 % to 70 % of their total sink at high liquid water content (LWC) (0.35 g m^{-3}). These results highlight the importance of investigating the aqueous-phase RONO_2 reactivity to understand how it affects their ability to transport air pollution.

1 Introduction

Organic nitrates play a key role in the formation, transport, and removal of NO_x . They are secondary compounds formed *via* $\text{NO}_x + \text{VOC}$ reactions. Depending on their structure, their lifetimes can be long (from a couple of hours to several days); thus they can be transported from polluted areas where they are formed to more remote areas (Shepson, 1999). During their long-range transport, these molecules are subject to reactions (i.e., gas-phase photolysis and/or $\bullet\text{OH}$ oxidation) re-

leasing back NO_x . RONO_2 are thus responsible for homogenizing the distribution of NO_x , and consequently, they impact other major pollutants such as O_3 and secondary organic aerosol (SOA) (Perring et al., 2013). Besides, RONO_2 can remove NO_x from the atmosphere by deposition to the Earth's surface or by transformation into a more inert chemical compound such as nitric acid (Hu et al., 2011; Nguyen et al., 2015). Therefore, their atmospheric reactivity and fate must be considered to accurately predict the transport of pollution on a regional scale. Besides, this is of special impor-

tance for world regions with decreasing NO_x levels (such as Europe and North America), where the RONO_2 relative importance as an NO_x reservoir and sink is increasing due to an increase in the overall rate of transformation of NO_x to RONO_2 (Romer Present et al., 2020).

Numerous studies have investigated the gas-phase reactivity of individual RONO_2 molecules (Suarez-Bertoa et al., 2012; Picquet-Varraut et al., 2020; Bedjanian et al., 2018; Talukdar et al., 1997a, b; Clemitshaw et al., 1997; Atkinson and Aschmann, 1989; Morin et al., 2016), mainly focusing on $\bullet\text{OH}$ oxidation and photolysis. Their results show that the kinetics and mechanisms of these reactions are highly influenced by the RONO_2 chemical structure. Although the presence of the nitrate group in the molecule hinders the $\bullet\text{OH}$ attack, $\bullet\text{OH}$ oxidation generally represents the main RONO_2 gas-phase sink (Shepson, 1999). However, RONO_2 with conjugated carbonyl groups are consumed faster *via* photolysis due to an enhancement in their light absorption. This is of high importance for ubiquitous biogenic RONO_2 such as isoprene and terpene RONO_2 which often bear conjugated carbonyl groups (Müller et al., 2014; Shen et al., 2021).

RONO_2 are not just present in the gas phase, as some of them are low volatile compounds and thus partition into condensed phases. As a result, they represent a fraction ranging from 5 % to 77 % of the submicron organic aerosol (Kiendler-Scharr et al., 2016; Ng et al., 2017). Under dry conditions, RONO_2 are dissolved in the aerosol phase where the matrix is mostly organic. With increasing relative humidity (RH), the particle can be covered by a water layer where RONO_2 (whether it comes from the particle or the gas phase) can partition. In this case, we consider that soluble RONO_2 partition to the aqueous phase where they exhibit a specific reactivity.

The aqueous-phase reactivity of RONO_2 plays a significant role in their atmospheric fate. The hydrolysis of tertiary and allylic RONO_2 represents a fast and permanent sink of NO_x in the atmosphere (Hu et al., 2011; Darer et al., 2011; Rindelaub et al., 2015). However, only a small fraction (between 9 % and 34 % for α - and β -pinene RONO_2) of the total pool of organic nitrates undergoes hydrolysis (Takeuchi and Ng, 2019; Wang et al., 2021). Aqueous-phase $\bullet\text{OH}$ oxidation has been reported to be an important sink for non-volatile terpene RONO_2 , even though the $\bullet\text{OH}$ attack is more effectively hindered in the aqueous phase than in the gas phase (González-Sánchez et al., 2021). Nevertheless, limited information is available for RONO_2 aqueous-phase photolysis. To our knowledge, only one study investigated the aqueous-phase absorption cross-sections of individual RONO_2 (Romonosky et al., 2015). However, the literature shows no aqueous-phase photolysis quantum yields, and thus no RONO_2 aqueous-phase photolysis-rate constants have been determined so far. Furthermore, the photolysis of RONO_2 with conjugated carbonyl groups remains unexplored, despite its high atmospheric relevance.

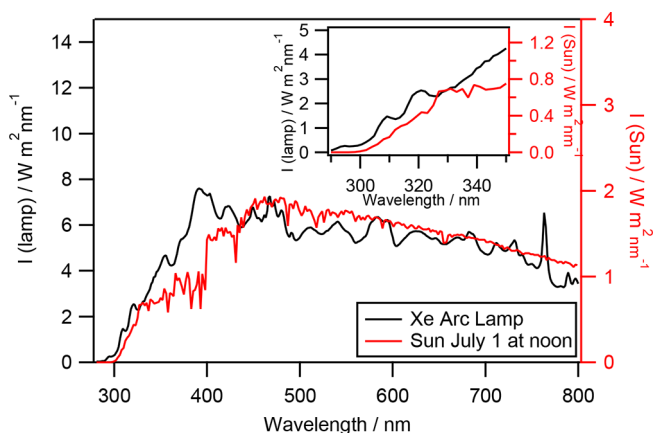


Figure 1. Irradiation spectra of the Xe 1000 W arc lamp equipped with an AM1.5 filter (black line) compared to the solar irradiation spectra (red line) on the 1 July 2015 at 40° latitude at ground level with an overhead ozone column of 300 DU and a surface albedo of 0.1 (using the tropospheric ultraviolet (TUV) model, Madronich and Flocke, 1999). Inner graph: zoom on the 290 to 350 nm region.

The objective of this work was to determine the aqueous-phase photolysis rate constants of individual RONO_2 including a carbonyl nitrate. Experimental photolysis-rate constants of four organic nitrates (isopropyl nitrate, isobutyl nitrate, α -nitrooxyacetone, and 1-nitrooxy-2-propanol) were determined in an aqueous-phase photoreactor, and their average aqueous-phase quantum yields were determined. Then, atmospheric aqueous-phase photolysis-rate constants were calculated under various realistic solar light conditions. Finally, using the experimental results, some estimations were performed for the aqueous-phase photolysis rate constants of a set of 45 atmospherically relevant RONO_2 , a global evaluation of all atmospheric sinks in both the gas and the aqueous phase was done, and their atmospheric lifetimes were estimated.

2 Materials and methods

2.1 Aqueous-phase photoreactor

The photolysis experiments were performed in a 450 cm³ double-wall Pyrex aqueous-phase photoreactor (Fig. S1; see details in Renard et al., 2013). The reactor was irradiated by an arc light source (LOT Quantum Design) equipped with a 1000 W arc Xe lamp. Irradiation below 290 nm was removed by an ASTM 892 AM1.5 standard filter. A constant distance (18.4 cm) between the lamp and the water surface was carefully maintained in all experiments using 400 mL of aqueous solution. The Xe arc lamp spectrum is presented in Fig. 1 (black line) and is compared to the solar actinic flux (red line) on the 1 July 2015 at 40° latitude at ground level. The lamp actinic flux that reaches the photoreactor was measured by an actinometry study with H_2O_2 (detailed in Supplement S1).

2.2 Experimental protocol and determination of experimental RONO_2 photolysis-rate constants

Before each photolysis experiment, the photoreactor was filled with 400 mL of ultrapure water and the investigated solubilized compound. The solution was stirred in the dark for 30 min for complete dissolution of the compound. In parallel, the lamp was lighted 10 min before the reaction started to stabilize the light beam. Once the reactor was placed underneath the light beam, the first aliquot was sampled signaling the reaction time zero. Photolysis reactions were performed for 7 h at 298.0 ± 0.2 K and “non-controlled” pH (without buffer solutions). During the reaction time, aliquots were sampled regularly (from 2 to 10 min) for offline UHPLC-UV analyses. All the performed photolysis experiments, including experimental conditions, and kinetic results are appended in Table S2.2. As shown in our previous study (González-Sánchez et al., 2021), isopropyl nitrate and isobutyl nitrate are subject to significant evaporation to the reactor’s headspace, and α -nitrooxyacetone is subject to hydrolysis. Therefore, control experiments (under dark conditions) were performed to subtract the evaporation and/or hydrolysis kinetic contributions (see Table S2.3). Furthermore, slight quantities of $\bullet\text{OH}$ radicals were formed during the photolysis experiments (via photolysis of the produced HNO_2 and NO_2^-). Since $\bullet\text{OH}$ radicals react with RONO_2 (González-Sánchez et al., 2021), their attack has been considered (Eq. 1) to precisely determine the RONO_2 aqueous-phase photolysis-rate constant.

$$\begin{aligned}\ln \frac{[\text{RONO}_2]_0}{[\text{RONO}_2]_t} &= k' \cdot t \\ &= \left(J_{\text{RONO}_2} + k_{\text{vap/hyd}} \right. \\ &\quad \left. + k_{\text{OH}} [\bullet\text{OH}] \right) \cdot t,\end{aligned}\quad (1)$$

where $[\text{RONO}_2]_0/[\text{RONO}_2]_t$ is the relative decay of aqueous-phase concentrations of the molecule; k' is the pseudo-first-order total decay-rate constant (s^{-1}); J_{RONO_2} is the experimental photolysis-rate constant (s^{-1}); k_{vap} and k_{hyd} are the experimental evaporation and hydrolysis-rate constants (s^{-1}), respectively; k_{OH} is the aqueous-phase $\bullet\text{OH}$ oxidation-rate constant ($\text{M}^{-1} \text{s}^{-1}$); $[\bullet\text{OH}]$ is the aqueous-phase $\bullet\text{OH}$ radical concentration (M); and t is time (s). A detailed explanation of the estimation of $\bullet\text{OH}$ radical concentration is given in Supplement (Sect. S2). Note that the contribution of the $\bullet\text{OH}$ oxidation varies with time, since $\bullet\text{OH}$ radicals were secondarily formed. Therefore, only data at the beginning of the reaction (< 2 h) were further employed to minimize this contribution. Under these conditions, aqueous-phase $\bullet\text{OH}$ oxidation of RONO_2 accounted for 5 % to 10 % of the total decay.

2.3 Analyses of aqueous solutions of RONO_2

The absorption cross-sections of RONO_2 and H_2O_2 in solution were determined from 190 to 340 nm with a UV-Vis-NIR double-beam spectrophotometer (JASCO V670). In addition to the four RONO_2 for which experimental photolysis-rate constants were investigated (isopropyl nitrate, isobutyl nitrate, α -nitrooxyacetone, and 1-nitrooxy-2-propanol), the absorption cross-sections of four additional RONO_2 were investigated (1-pentyl nitrate, isopentyl nitrate, 2-ethylhexyl nitrate, and isosorbide 5-mononitrate). Due to low absorption cross-sections above 290 nm, a 5 cm path-length cell was used, and due to the low water solubility of some RONO_2 , a methanol or methanol and water mixture was used as a solvent. The solvents’ effects on the absorption cross-sections were investigated for isopropyl nitrate. Table S1 lists the solvents and ranges of concentrations used to investigate the absorption cross-sections of each RONO_2 (and also H_2O_2).

The investigated organic nitrates showed an intense UV absorption band around 200 nm (Fig. S2). During the photolysis experiments, isopropyl nitrate, isobutyl nitrate, α -nitrooxyacetone, and 1-nitrooxy-2-propanol were monitored by UHPLC-UV. The instrument was a Thermo Scientific Accela 600 equipped with a Hypersil Gold C18 column (50×2.1 mm) with a particle size of $1.9 \mu\text{m}$ and an injection loop of $5 \mu\text{L}$ at 200 nm. A binary eluent of H_2O and CH_3CN was used for all analyses at a flow rate of $400 \mu\text{L min}^{-1}$. Two gradients were used depending on the compounds’ polarity. For α -nitrooxyacetone and 1-nitrooxy-2-propanol, the gradient started from $\text{H}_2\text{O} / \text{CH}_3\text{CN}$ 90/10 (v/v) to 50/50 (v/v) for 3 min, held at this proportion for 1 min, and then set back to 90/10 (v/v) within 10 s until the end of the run, at minute 5. For isopropyl nitrate and isobutyl nitrate, a similar gradient was employed, but the initial and final proportions were $\text{H}_2\text{O} / \text{CH}_3\text{CN}$ 80/20 (v/v).

Calibration curves were optimized to obtain good linearity between 5×10^{-5} and 1×10^{-3} M with an $R^2 > 0.9995$. The retention times were 0.9, 1.2, 2.4, and 3.3 min for 1-nitrooxy-2-propanol, α -nitrooxyacetone, isopropyl nitrate, and isobutyl nitrate, respectively. Limits of detection were 1×10^{-5} M for 1-nitrooxy-2-propanol and α -nitrooxyacetone and 9×10^{-6} M for isopropyl nitrate and isobutyl nitrate.

2.4 Reagents

Chemicals were commercially available and used as supplied: isopropyl nitrate (96 %; Sigma Aldrich), isobutyl nitrate (98 %; Sigma Aldrich), 2-ethylhexyl nitrate (97 %; Sigma Aldrich), 1-pentyl nitrate (98 %; TCI Chemicals), isopentyl nitrate (98 %; TCI Chemicals), isosorbide 5-mononitrate (98 %; Acros Organics), and H_2O_2 (30 %; non-stabilized, Acros Organics). Non-commercially RONO_2 , α -nitrooxyacetone, and 1-nitrooxy-2-propanol were synthesized and purified (see Supplement Sect. S3). LC/MS grade

acetonitrile (Fisher Optima) was used as supplied. Tap water was purified with a Millipore MiliQ system (18.2 M Ω cm and TOC <2 ppb).

3 Results and discussions

3.1 Liquid-phase absorption cross-sections of RONO₂

UV-Vis absorbance was investigated for eight organic nitrates (i.e., isopropyl nitrate, isobutyl nitrate, 1-pentyl nitrate, isopentyl nitrate, 2-ethylhexyl nitrate, α -nitrooxyacetone, 1-nitrooxy-2-propanol, and isosorbide 5-mononitrate) dissolved in water or methanol. All RONO₂ absorbed UV light between 190 and 330 nm, with maximum absorption at 210 nm due to the $\pi \rightarrow \pi^*$ transition (see Fig. S2). At longer wavelengths, the absorption is produced due to an $n \rightarrow \pi^*$ transition. This transition appears as a shoulder of the $\pi \rightarrow \pi^*$ transition and extends up to ~ 330 nm. The $n \rightarrow \pi^*$ transition is responsible for the light absorption at $\lambda \geq 290$ nm and thus is relevant for the atmospheric photolysis of RONO₂. The determination of the liquid-phase absorption cross-sections of RONO₂ is detailed in the Supplement (Sect. S4), and all values are compiled in Table S2.

3.1.1 Liquid-phase absorption cross-sections of alkyl nitrates

Figure 2 shows the absorption cross-sections determined for all investigated alkyl nitrates and are compared to those reported in the literature (both in the liquid and the gas phase). Since the absorption cross-sections of alkyl nitrates were mostly investigated in methanol due to their low water solubilities, the absorption cross-sections of isopropyl nitrate in water have been compared to that in methanol. The comparison showed that there is a slight shift to shorter wavelengths (blue shift) when isopropyl nitrate is dissolved in water (~ 5 nm in the most impacted region). This shift is likely caused by the stabilization of the non-bonding orbital with increasing solvent polarity. Since this stabilization lowers the ground-state energy, the $n \rightarrow \pi^*$ transition energy increases, and thus shorter wavelengths are needed to promote the electron.

It can be concluded from Fig. 2 that all the investigated alkyl nitrates showed similar absorption cross-sections in the liquid phase. The absorption cross-sections determined for isopropyl nitrate are in good agreement with those determined by Romonosky et al. (2015). However, for 2-ethylhexyl nitrate, slightly lower values were obtained in this work at $\lambda < 300$ nm, even though a more polar solvent was used in our work, the reason for this difference is not clear.

Compared to the gas-phase absorption cross-sections, isobutyl nitrate and 1-pentyl nitrate present a $\sim 40\%$ increase in solution. For isopropyl nitrate this increase is less important; the absorption cross-sections are $\sim 25\%$ higher in methanol and nearly identical in water.

3.1.2 Liquid-phase absorption cross-sections of polyfunctional RONO₂

Figure 3 shows the absorption cross-sections determined for the investigated polyfunctional RONO₂ dissolved in water or water and methanol. 1-Nitrooxy-2-propanol (Fig. 3b) and isosorbide 5-mononitrate (Fig. 3c) presented absorption cross-section values similar to the investigated alkyl nitrates (Fig. 2). In contrast, α -nitrooxyacetone absorption cross-sections (Fig. 3a) were around 5 times higher (note the different scale used for this molecule) due to the conjugation of the carbonyl and the nitrooxy group. Furthermore, there are differences in the shape of its spectra: a large shoulder is observed from 320 to 390 nm. This band is not observed in the gas phase, and thus it might be caused by interactions between the two chemical groups and the solvent, or it could correspond to an impurity that remained after synthesis, even after purification.

For isosorbide 5-mononitrate absorption cross-sections, the values observed in this work were similar to those determined by Romonosky et al. (2015), although our values were slightly lower at $\lambda > 310$ nm.

Comparison between liquid- and gas-phase absorption cross-sections show that UV absorption is significantly enhanced when polyfunctional RONO₂ are in solution. For α -nitrooxyacetone, this enhancement is of a factor of 2 compared to the values determined by Barnes et al. (1993) and Roberts and Fajer (1989).

The absorption cross-sections of 1-nitrooxy-2-propanol have not been investigated in the gas phase. Figure 3b compares its aqueous-phase absorption cross-sections with those of gas-phase 1-nitrooxyethanol (in red in Fig. 3b), determined by Roberts and Fajer (1989). The only other β -hydroxy RONO₂ for which gas-phase absorption cross-sections were investigated, i.e., *trans*-2-nitrooxy-1-cyclopentanol, is not shown here, since the molecule does not absorb UV light above 275 nm (Wängberg et al., 1996).

Figure 3d displays the absorption cross-sections of six additional β -hydroxy RONO₂ (listed in Table 2) in solution. Overall, Fig. 3b and d show that the absorption cross-sections are higher by an order of magnitude for molecules in solution compared to the gas phase. These observations suggest that the nitrate group absorption is likely hindered by the hydroxy group in the gas phase but not in solution, probably due to solvent effects. Nevertheless, gas-phase absorption cross-sections should be determined for other hydroxy RONO₂ to confirm this hypothesis. This is of special atmospheric relevance, since β -hydroxy nitrates are formed *via* the addition of \bullet OH radicals to atmospherically relevant unsaturated molecules (such as terpene nitrates and aromatic nitrates, for example) and may significantly partition between the gas and the condensed phases in the atmosphere.

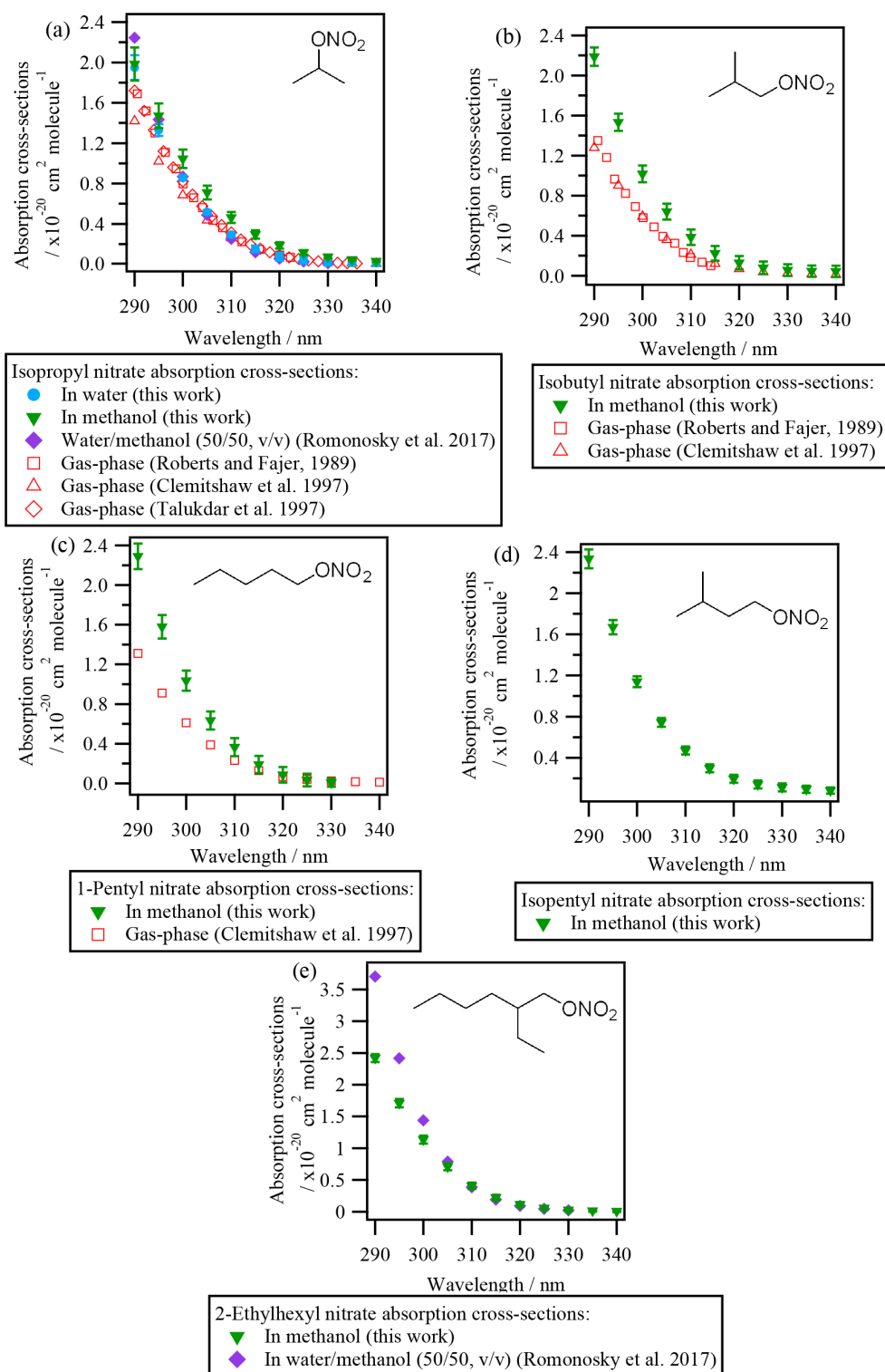


Figure 2. Absorption cross-sections of alkyl nitrates in methanol and/or water. Gas-phase absorption cross-sections are included (in red) when available (for isopropyl nitrate, isobutyl nitrate, and 1-pentyl nitrate).

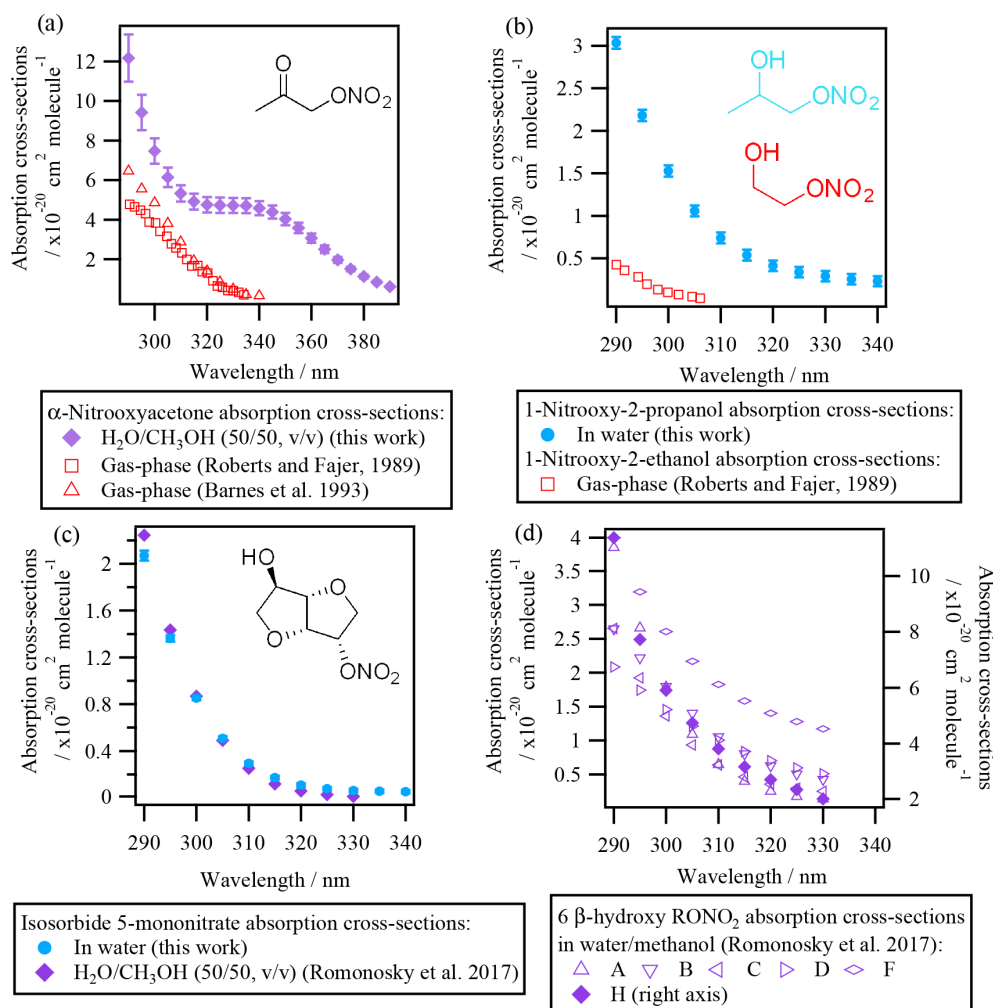


Figure 3. Absorption cross-sections of polyfunctional RONO_2 in water or water and methanol determined in this work and in Romonosky et al. (2015). Gas-phase absorption cross-sections of polyfunctional RONO_2 are included when available (for α -nitrooxyacetone and 2-nitrooxyethanol). β -Hydroxy nitrates A, B, C, D, F, and H are listed in Table 2.

3.2 Liquid-phase photolysis quantum yields of RONO_2

The photolysis quantum yields of RONO_2 were estimated in the liquid phase for the first time. For that purpose, the maximum theoretical photolysis-rate constants of RONO_2 were calculated assuming quantum yields of unity and then compared with the experimentally determined ones.

The maximum theoretical photolysis-rate constants of RONO_2 under our experimental conditions were calculated using Eq. (2):

$$J_{\text{calc}} = \int \sigma(\lambda) \Phi(\lambda) I(\lambda) d\lambda, \quad (2)$$

where J_{calc} is the calculated photolysis-rate constant (s^{-1}), $I(\lambda)$ is the corrected lamp actinic flux ($\text{photons s}^{-1} \text{cm}^{-2} \text{nm}^{-1}$), and $\Phi(\lambda)$ is the quantum yield (assumed equal to one). Since the calculated values represented maximum-rate constants using liquid-phase quantum yields

of unity, Eq. (3) has been used to estimate the actual quantum yields, assuming a constant value over 290–340 nm.

$$\Phi = \frac{J_{\text{exp}}}{J_{\text{calc}}}, \quad (3)$$

where J_{exp} is the experimental-rate constant (s^{-1} ; Table 1).

Quantum yields are given only for isopropyl nitrate, isobutyl nitrate, α -nitrooxyacetone, and 1-nitrooxy-2-propanol (investigated for J_{exp}). Furthermore, for each molecule, while quantum yields may vary with λ , an average quantum yield was determined over atmospherically relevant wavelengths (290 to 340 nm). Wavelength-resolved quantum yields might be important for α -nitrooxyacetone, since two distinct absorbance bands were observed at the investigated wavelengths (Fig. 3). Additionally, isobutyl nitrate and α -nitrooxyacetone photolysis-rate constants might be overestimated due to the solvent used for the determinations of their absorption cross-sections. Indeed, for isopropyl nitrate,

a 60 % increase in the calculated photolysis-rate constant was observed when dissolved in methanol as compared to water (Table 1). However, no corrections were performed for isobutyl nitrate and α -nitrooxyacetone, since the enhancement reported for isopropyl nitrate cannot be generalized to other molecules.

Table 1 shows the calculated and experimental photolysis-rate constants along with the estimated quantum yields. It clearly shows that the maximum calculated values (J_{calc}) were similar for all compounds, except for 1-nitrooxy-2-propanol and α -nitrooxyacetone. These compounds presented much higher values due to their stronger UV absorption. In contrast, the aqueous-phase experimental photolysis-rate constants were of the same order of magnitude for the four investigated RONO₂, and no increase associated with the presence of any functional group adjacent to the nitrate group was observed.

Table 1 also shows that quantum yields are much lower in the liquid phase than in the gas phase. The estimated quantum yields are ~ 3 , ~ 15 , and ~ 500 times lower in solution for alkyl nitrates, 1-nitrooxy-2-propanol, and α -nitrooxyacetone, respectively. This observation is coherent with previous studies showing that the photolysis quantum yields in the aqueous phase are usually lower than those in the gas phase, as shown, for example, for H₂O₂ or HNO₃ (Herrmann, 2007; Bianco et al., 2020; Romer et al., 2018). This can be caused by the solvent cage effect. When a molecule is photolyzed in a solvent, its photolysis products are trapped by the surrounding solvent molecules. This solvent cage eases the reconversion of the products into the original molecule and thus decreases the overall quantum yield. Additionally, excited molecules can easily lose the gained energy by colliding with the surrounding solvent molecules.

Although the absorption cross-sections of polyfunctional RONO₂ such as α -nitrooxyacetone and 1-nitrooxyacetone are enhanced in solution, the enhancement does not imply an increase in their photolysis-rate constants, since their quantum yields are also lower in solution. The same effect has been reported for the photolysis of NO₃[−] in bulk aqueous solutions when compared to the gas-phase photolysis of HNO₃ (Svoboda et al., 2013; Warneck and Wurzinger, 1988; Nissen et al., 2010).

For α -nitrooxyacetone, the extremely low quantum yield determined in this work is influenced by the important absorption band observed above 320 nm (Fig. 3). However, even when removing this band from its absorption cross-sections (by deconvolution of the spectra; see Supplement Sect. S5), a very low quantum yield was obtained (0.02), lower than any other RONO₂ due to its higher absorption between 290 and 320 nm. In any case, the aqueous-phase photolysis-rate constant of this compound was similar to the other RONO₂ despite its much higher UV absorption. This is of special importance, since gas-phase photolysis is one of the major sinks for carbonyl RONO₂ (Müller et al., 2014). These results indicate that if these compounds effectively

partition to the aqueous phase, their photolysis may not be such a relevant sink.

To evaluate the atmospheric impact of aqueous-phase photolysis, its rate constants were calculated under various light conditions for the investigated organic nitrates and seven other RONO₂ molecules for which liquid-phase absorption cross-sections were reported by Romonosky et al. (2015).

3.3 Atmospheric aqueous-phase photolysis-rate constants of RONO₂

Atmospheric aqueous-phase photolysis-rate constants were calculated for 14 RONO₂ using Eq. (2) under two different scenarios (Table 2): (i) a global scenario (actinic flux with a 60° solar zenith angle), and (ii) a summer scenario (actinic flux for the 1 July at noon at 40° latitude). The latter was investigated to determine the maximum aqueous-phase photolysis kinetics of RONO₂ under atmospheric conditions. The actinic flux was taken from the tropospheric ultraviolet visible (TUV) model (Madronich and Flocke, 1999). Other parameters in common for both scenarios were an overhead ozone column of 300 DU, a surface albedo of 0.1, and a ground elevation of 0 km. Although it has been discussed that light is enhanced in liquid cloud droplets by a factor of 2 (Madronich, 1987), this enhancement factor was not included here, since it can largely fluctuate. Furthermore, the comparison with the gas-phase photolysis-rate constants appears clearer if no enhancement factor is included.

The investigated RONO₂ comprised five alkyl nitrates, one ketonitrate, and eight hydroxy nitrates, out of which seven are β -hydroxy nitrates, and four of them conjugate more than one functional group. The absorption cross-sections were either calculated in this work or taken from Romonosky et al. (2015) who determined the absorption cross-sections of several RONO₂ compounds dissolved in a mixture of water and methanol (50/50, *v/v*). Using our results shown above (Table 1), a quantum yield of 0.34 (average from isopropyl nitrate and isobutyl nitrate) was applied to all alkyl nitrates and isosorbide 5-mononitrate, a quantum yield of 0.07 was applied for all β -hydroxy nitrates, and a quantum yield of 0.002 was applied for α -nitrooxyacetone.

The aqueous-phase photolysis lifetimes were estimated using Eq. (4).

$$\tau_{hv} = \frac{1}{J_{\text{aq}} \cdot 86400}, \quad (4)$$

where τ_{hv} is the aqueous-phase photolysis lifetime (in days), and J_{aq} is the aqueous-phase photolysis-rate constant (in s^{−1}).

Table 2 shows that all aqueous-phase photolysis-rate constants were similar except for α -nitrooxyacetone and the molecule labeled H. For the latter, absorption cross-sections (determined by Romonosky et al., 2015) were higher than for all the other investigated RONO₂ (Fig. 3), probably due to the conjugated ester and vinyl groups in the molecule. Likely,

Table 1. Calculated and experimental photolysis-rate constants of RONO_2 in the liquid phase, estimated liquid-phase quantum yields (Φ), and comparison with gas-phase Φ .

RONO_2	Solvent for J_{calc}	J_{calc} ($\times 10^{-5} \text{ s}^{-1}$)	J_{exp} ($\times 10^{-5} \text{ s}^{-1}$)	Liquid-phase Φ	Gas-phase Φ
Isopropyl nitrate	water	1.69 ± 0.43	0.50 ± 0.10	0.29 ± 0.09	$1.00 \pm 0.05^{\text{a}}$
	methanol	2.86 ± 0.38			
Isobutyl nitrate	methanol	2.43 ± 0.89	0.94 ± 0.34	0.39 ± 0.20	1^{c}
1-Pentyl nitrate	methanol	1.92 ± 0.69			
Isopentyl nitrate	methanol	3.30 ± 0.52			
2-Ethylhexyl nitrate	methanol	2.31 ± 0.41			
Isosorbide 5-mononitrate	water	2.12 ± 0.20			
1-Nitrooxy-2-propanol	water	6.16 ± 0.85	0.40 ± 0.04	0.07 ± 0.01	1^{c}
α -Nitrooxyacetone	water and methanol	172 ± 16	0.31 ± 0.02	0.002 ± 0.001	0.9^{b}

^a Experimentally determined at 308, 315, and 320 nm by Carbajo and Orr-Ewing (2010). ^b Estimated by Müller et al. (2014) out of data from Suarez-Bertoa et al. (2012). ^c Assumed to be similar to alkyl nitrates gas-phase Φ .

this molecule presents a quantum yield lower than 0.07, and thus its photolysis-rate constant was probably overestimated in Table 2. Furthermore, although slight differences were observed between this work and that of Romonosky et al. (2015) for isopropyl nitrate and 2-ethylhexyl nitrate, significant differences were obtained for isosorbide 5-mononitrate. This is due to slightly higher determined absorption cross-sections between 310 and 340 nm (Fig. 3). At these wavelengths, the high intensity of the solar actinic flux provokes a substantial variation in the photolysis-rate constants.

The apparent similarities between all the RONO_2 aqueous-phase photolysis-rate constants are of special importance, since they indicate that RONO_2 molecules show very similar aqueous-phase photolysis lifetimes irrespective of the functional group besides the nitrate function.

Table 2 shows that, in general, aqueous-phase global photolysis lifetimes are quite long (from 6 to 210 d), and thus RONO_2 can remain in the aqueous phase for several days if they do not hydrolyze or undergo other sinks. The aqueous-phase photolysis lifetimes are shortened by a factor between 2.4 and 3.5 when using a solar spectrum at noon on the 1 July.

The comparison between the aqueous-phase and the gas-phase photolysis lifetimes shows that alkyl nitrate lifetimes are relatively similar. However, strong deviations are observed for α -nitrooxyacetone and 1-nitrooxy-2-propanol.

α -Nitrooxyacetone presents a much longer photolysis lifetime in the aqueous phase (210 vs. 0.9 d) due to the extremely low photolysis quantum yield in the aqueous phase (0.002). This implies that the aqueous-phase photolysis is a negligible sink for α -nitrooxyacetone. As mentioned above, gas-phase photolysis is the major sink for carbonyl nitrates as their kinetics are enhanced by the conjugation of the nitrate and the carbonyl group. Our results show that this enhancement is hindered in the aqueous phase, and thus photolysis might not be the major sink for carbonyl nitrates partitioning to the aqueous phase.

Conversely, the pair of β -hydroxynitrates compared (1-nitrooxy-2-propanol and 2-nitrooxyethanol) show a much shorter lifetime in the aqueous phase (16 vs. 2400 d) due to a large increase in the absorption cross-sections (Fig. 3). Therefore, the photolysis sink of β -hydroxynitrates is likely greatly enhanced if they partition to the atmospheric aqueous phase. Nevertheless, the obtained very long lifetimes suggest that aqueous-phase photolysis remains a negligible sink.

To investigate the relative importance of the aqueous-phase photolysis in the RONO_2 atmospheric fate, the multiphase lifetimes of several atmospherically relevant RONO_2 were calculated, as exposed in the next section.

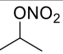
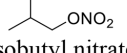
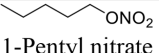
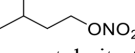
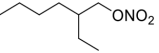
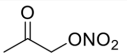
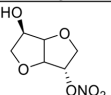
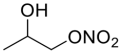
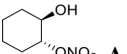
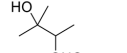
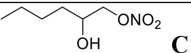
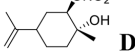
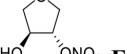
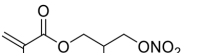
4 Atmospheric implications

4.1 Photochemical sink contributions to RONO_2 multiphase lifetimes

Multiphase photochemical lifetimes were calculated for 32 non-hydrolyzable atmospherically relevant RONO_2 classified in three families according to their VOC precursor and water solubility: 6 small RONO_2 (isopropyl nitrate, isobutyl nitrate, 1-pentyl nitrate, isopentyl nitrate, 1-nitrooxy-2-propanol, and nitrooxyacetic acid) with low to intermediate water solubilities ($K_{\text{H}} \sim 10^{-1}$ to 10^5 M atm^{-1}), 5 isoprene nitrates (ethanal nitrate, α -nitrooxyacetone, two methyl vinyl ketone nitrate isomers, and a C_5 dihydroxy dinirate) with intermediate to high water solubilities ($K_{\text{H}} \sim 10^3$ to 10^7 M atm^{-1}), and 12 terpene nitrates (α - and β -pinene, limonene, γ -terpinene, and myrcene atmospheric reactivity products) with intermediate to very high water solubilities ($K_{\text{H}} \sim 10^4$ to $10^{12} \text{ M atm}^{-1}$). The chemical structures of the investigated RONO_2 and their Henry's law constants are listed in Table S3.

In the same manner as in González-Sánchez et al. (2021), the multiphase photochemical lifetimes were investigated under two different scenarios: (i) under cloud and fog condi-

Table 2. Calculated aqueous-phase photolysis-rate constants and lifetimes for a series of RONO_2 under two scenarios (global and summer) and comparison with their gas-phase values.

RONO_2	Aqueous phase				Gas phase	
	J_{global} ($\times 10^{-7} \text{ s}^{-1}$)	$\tau_{\text{hv,global}}$ (d)	J_{summer} ($\times 10^{-7} \text{ s}^{-1}$)	$\tau_{\text{hv,summer}}$ (d)	J_{global} ($\times 10^{-7} \text{ s}^{-1}$)	$\tau_{\text{hv,global}}$ (d)
 Isopropyl nitrate	3.2 ^a 4.2 ^b	36 27	10 14	12 8	8.9 ^c	14
 Isobutyl nitrate	5.9 ^a	20	17	7	5.3 ^d	22
 1-Pentyl nitrate	3.0 ^a	38	11	11	8.9 ^c	13
 Isopentyl nitrate	9.7 ^a	12	25	5		
 2-Ethyl hexyl nitrate	4.4 ^a 3.5 ^b	26 33	14 12	8 10		
 α -Nitrooxyacetone	0.56 ^a	210	1.4	77	129 ^f	0.9
 Isosorbide 5-mononitrate	5.6 ^a 2.1 ^b	21 54	15 7.5	8 16		
 1-Nitrooxy-2-propanol	4.2 ^a	27	10	11	0.05 ^g	2400
 A	1.8 ^b	66	5.1	23		
 B	4.2 ^b	27	11	10		
 C	2.5 ^b	47	6.6	18		
 D	4.7 ^b	25	12	10		
 F	9.7 ^b	12	24	5		
 H	18 ^b	6	47	2		

Aqueous-phase absorption cross-sections determined in ^a this work and ^b Romonosky et al. (2015). Average gas-phase absorption cross-sections are taken from ^c Clemitshaw et al. (1997), Roberts and Fajer (1989), and Talukdar et al. (1997). ^d Clemitshaw et al. (1997) and Roberts and Fajer (1989). ^e Clemitshaw et al. (1997). ^f Barnes et al. (1993) and Roberts and Fajer (1989). ^g The value from Roberts and Fajer (1989) corresponding to 2-nitrooxyethanol.

tions (liquid water content $\text{LWC} = 0.35 \text{ g m}^{-3}$), and (ii) under wet aerosol conditions ($\text{LWC} = 3 \times 10^{-5} \text{ g m}^{-3}$), using Eq. (5):

$$\tau_{\text{multiphase}} = \frac{1}{\varphi_{\text{aq}} \cdot J_{\text{aq}} + \varphi_{\text{aq}} \cdot k_{\text{OH, aq}} \cdot [\text{OH}]_{\text{aq}} + \varphi_{\text{gas}} \cdot J_{\text{gas}} + \varphi_{\text{gas}} \cdot k_{\text{OH, gas}} \cdot [\text{OH}]_{\text{gas}}}, \quad (5)$$

where φ_{aq} and φ_{gas} is the molar fraction of the compound in the aqueous and the gas phase, respectively; J_{aq} and

J_{gas} (s^{-1}) are the global photolysis-rate constants (actinic flux with a 60° solar zenith angle) in the aqueous and the gas phase, respectively; $k_{\text{OH, aq}}$ and $k_{\text{OH, gas}}$ (in $\text{M}^{-1} \text{ s}^{-1}$ and $\text{cm}^3 \text{ molec.}^{-1} \text{ s}^{-1}$, respectively) are the aqueous and gas-phase $\bullet\text{OH}$ oxidation-rate constants; and $[\text{OH}]_{\text{aq}}$ and $[\text{OH}]_{\text{gas}}$ (in M and molec. cm^{-3} , respectively) are the $\bullet\text{OH}$ concentrations in each phase.

The calculation of the aqueous- and gas-phase partitioning is detailed in Sect. S6.1, where each photolysis and $\bullet\text{OH}$ oxidation-rate constant assignments is explained in detail. Briefly, experimental values were used when available; otherwise, they were calculated using group contribution methods (González-Sánchez et al., 2021; Jenkin et al., 2018) or they were assumed based on experimental values of RONO_2 with similar chemical structures. The $\bullet\text{OH}$ concentrations were set to 10^{-14} M in the aqueous phase and 1.4×10^6 molec. cm^{-3} in the gas phase (Tilgner et al., 2013). All K_H values are set at 298 K as well as all reactivity kinetic-rate constants for which most of the activation energies are unknown. Note that lower temperatures should be more realistic, they should mostly affect K_H values; therefore, our results probably underestimate the atmospheric fractioning to the aqueous phase.

Figure 4 depicts the RONO_2 multiphase lifetimes under both cloud and fog conditions (Fig. 4a) and wet aerosol conditions (Fig. 4b). The chosen RONO_2 were distributed into three groups according to their nature and source and plotted by increasing water solubility. Figure 4 also shows the aqueous molar fraction of each molecule (in blue) and the relative contribution of each of the investigated sinks to the total multiphase lifetime.

Figure 4 shows much longer multiphase photochemical atmospheric lifetimes for small RONO_2 (from 38 to 264 h) than for isoprene and terpene nitrates (from 2 to 29 h). This is mainly due to their low number of $\bullet\text{OH}$ attack reactive sites and the absence of highly reactive groups such as aldehyde groups (fast $\bullet\text{OH}$ oxidation) or conjugated carbonyl groups (fast gas-phase photolysis).

The figure also highlights the relevance of aqueous-phase $\bullet\text{OH}$ oxidation, which is the only photochemical sink for RONO_2 partitioning into the aqueous phase. Photolysis is a negligible sink in the aqueous phase, whereas it is an important sink in the gas phase, especially for compounds bearing conjugated carbonyl groups (marked with * in the figure).

Figure 4 also shows that RONO_2 multiphase photochemical atmospheric lifetimes can substantially vary under different atmospheric LWC. RONO_2 lifetimes generally increase when the compound effectively partitions to the aqueous phase. This increase is especially important for compounds bearing conjugated carbonyl groups due to the significant difference in their photolysis kinetics between the gas and the aqueous phase. In the gas phase, photolysis is their major sink, while it becomes a minor or even negligible sink when they partition to the aqueous phase. Besides, RONO_2 with no conjugated carbonyl groups tend to show a mild increase in their lifetimes when partitioning to the aqueous phase caused by the deactivation of their $\bullet\text{OH}$ reactivity in water (González-Sánchez et al., 2021).

Comparing Fig. 4a and b, very different behaviors are observed depending on the RONO_2 Henry's law constant. The lifetimes of RONO_2 with low water solubilities ($K_H < 10^4$ M atm^{-1} ; i.e., RONO_2 with $\varphi_{\text{aq}} \leq 7\%$ in Fig. 4a) barely vary between the cloud and fog and the wet aerosol

scenarios, since their aqueous-phase molar fractions are extremely low.

In contrast, for molecules with intermediate to high water solubilities ($K_H = 10^5 - 10^9$ M atm^{-1} ; i.e., methyl vinyl ketone isomers, C_5 dihydroxy dinitrate, α -pinene 2–4, β -pinene 2–8, and terpinene 1), significant variations between the two scenarios are clearly observed. Their aqueous-phase partitioning ranges from 91 % (on average) under cloud and fog conditions to 12 % (on average) under wet aerosol conditions. Compared to wet aerosol conditions, the increase of photochemical lifetimes under cloud and fog conditions is much more pronounced for RONO_2 -bearing conjugated carbonyl groups (lifetimes up to 3 times higher) due to their much slower aqueous-phase reactivity.

Finally, very high water-soluble RONO_2 ($K_H \geq 10^{10}$ M atm^{-1} , i.e., RONO_2 for which $\varphi_{\text{aq}} \geq 89\%$ in Fig. 4b) barely partition to the gas phase even under low LWC, and thus their lifetimes are similar under both conditions. For these RONO_2 , aqueous-phase $\bullet\text{OH}$ oxidation is the main sink, even under wet aerosol conditions with extremely low amounts of water.

4.2 Importance of hydrolysis in multiphase chemical lifetimes

Hydrolysis is a known process that can influence the atmospheric lifetimes of RONO_2 , mostly tertiary and allylic RONO_2 . These chemical structures can stabilize the reaction of intermediate carbocation formed through the acid-catalyzed unimolecular nucleophilic substitution ($\text{S}_{\text{N}}1$). Other RONO_2 (such as primary or secondary RONO_2) can also undergo hydrolysis under very acidic conditions (Rindelaub et al., 2016; Wang et al., 2021), but these reactions remain extremely slow under atmospheric conditions, and they are considered in this work as “non-hydrolyzable”.

Up to date, the hydrolysis of nine tertiary RONO_2 and four allylic RONO_2 have been experimentally investigated by different authors (Hu et al., 2011; Darer et al., 2011; Jacobs et al., 2014; Rindelaub et al., 2015; Wang et al., 2021), reporting a wide range of hydrolysis-rate constants at neutral pH (from 9.9×10^{-6} to 9.3×10^{-3} s^{-1}).

To assess the relative importance of aqueous-phase $\bullet\text{OH}$ oxidation and photolysis in relation to hydrolysis, the multiphase lifetimes of these RONO_2 were evaluated under the two scenarios (cloud and fog and wet aerosol conditions) using Eq. (6).

$$\tau_{\text{multiphase}} = \frac{1}{\varphi_{\text{aq}} \cdot k_{\text{hyd}} + \varphi_{\text{aq}} \cdot J_{\text{aq}} + \varphi_{\text{aq}} \cdot k_{\text{OH, aq}} \cdot [\text{OH}]_{\text{aq}} + \varphi_{\text{gas}} \cdot J_{\text{gas}} + \varphi_{\text{gas}} \cdot k_{\text{OH, gas}} \cdot [\text{OH}]_{\text{gas}}} \quad (6)$$

The chemical structures of the investigated compounds are described in Table S4 along with their Henry's law constants (from 1 to 10^{10} M atm^{-1}) and their hydrolysis-rate constants. Assumptions performed to assign photolysis and $\bullet\text{OH}$ oxidation-rate constants are detailed in Sect. S6.2.

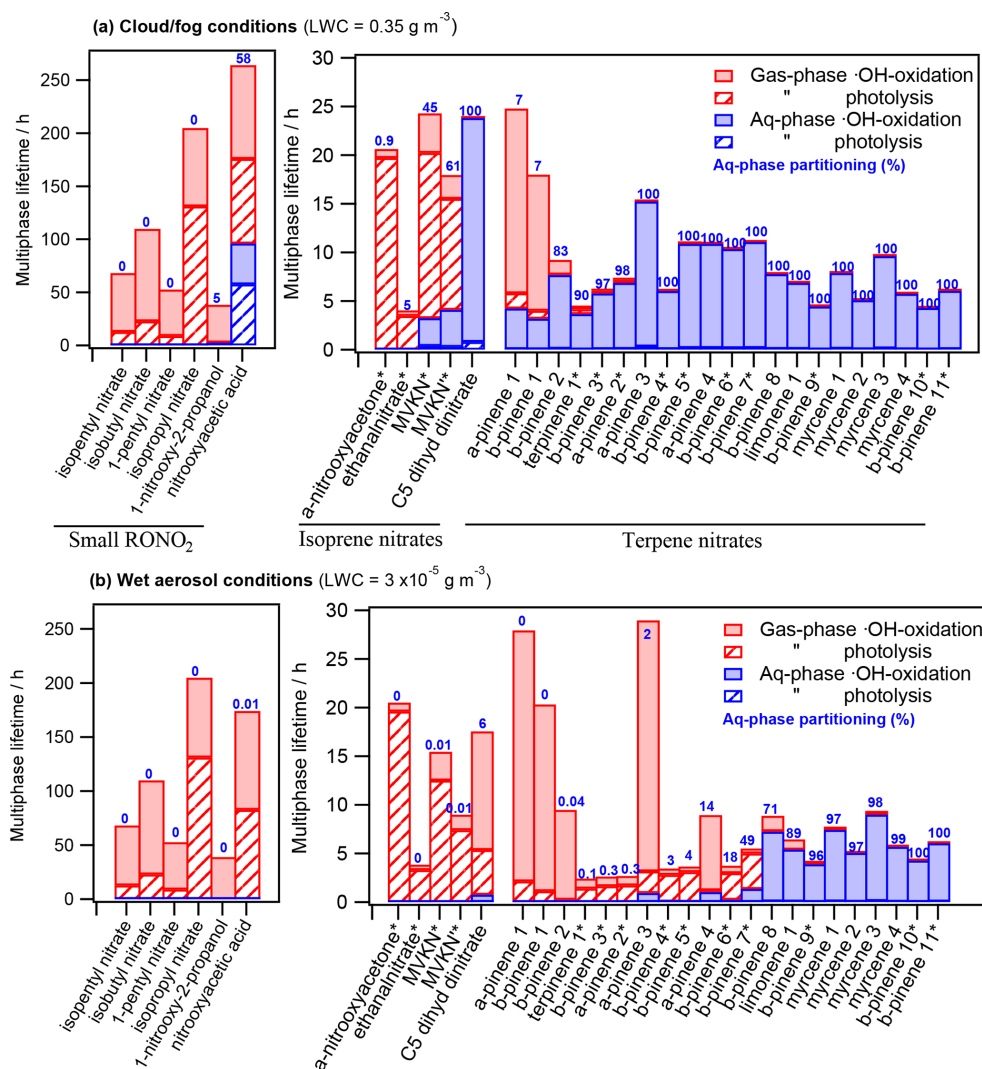


Figure 4. Chemical multiphase lifetimes and relative contribution of each sink for 32 atmospherically relevant RONO_2 distributed into (i) small RONO_2 (SN; left axis), (ii) isoprene nitrates (IN; right axis), and (iii) terpene nitrates (TN; right axis) under **(a)** cloud and fog conditions ($LWC = 0.35 \text{ g m}^{-3}$) and **(b)** wet aerosol conditions ($LWC = 3 \times 10^{-5} \text{ g m}^{-3}$). The numbers in blue indicate the aqueous-phase molar fraction (in %). * Conjugated carbonyl nitrates. The chemical structures, properties, and kinetic-rate constants of each compound are listed in Table S3.

Figure 5 displays the hydrolyzable RONO_2 multiphase atmospheric lifetimes in the same manner as in Fig. 4, and it shows that hydrolysis can substantially impact RONO_2 atmospheric removal.

On the one hand, for RONO_2 with high hydrolysis-rate constants (*tert* 3, 4, 7, 8, and 9 and *ally* 3 and 4 with $k_{\text{hyd}} > 10^{-3} \text{ s}^{-1}$), the hydrolysis is the major sink under cloud and fog conditions even for compounds that barely partition to the aqueous phase (*tert* 3 and 4), while under wet aerosol conditions, it can be a very significant sink (*tert* 7, 8, and 9). These RONO_2 are processed within less than 2 h under cloud and fog conditions, and their atmospheric lifetimes can be shortened by 2 orders of magnitude with respect to the wet aerosol scenario (only the highly water-soluble *tert* 9

presents similar lifetimes (0.7 h) under both conditions). For these RONO_2 , aqueous-phase $\cdot\text{OH}$ oxidation and photolysis are completely irrelevant, and their chemical lifetimes are only driven by hydrolysis or gas-phase reactivity depending on their atmospheric partitioning and hydrolysis-rate constants.

On the other hand, for RONO_2 with lower hydrolysis-rate constants ($k_{\text{hyd}} < 10^{-4} \text{ s}^{-1}$), aqueous-phase $\cdot\text{OH}$ oxidation can compete with or overcome hydrolysis as a faster sink (*tert* 6 and *ally* 1 and 2 under cloud and fog conditions). Nevertheless, their atmospheric removal is mostly controlled by their gas-phase reactivity due to their low water solubility. However, it is likely that the aqueous-phase $\cdot\text{OH}$ oxidation is an important process for other tertiary and allylic RONO_2

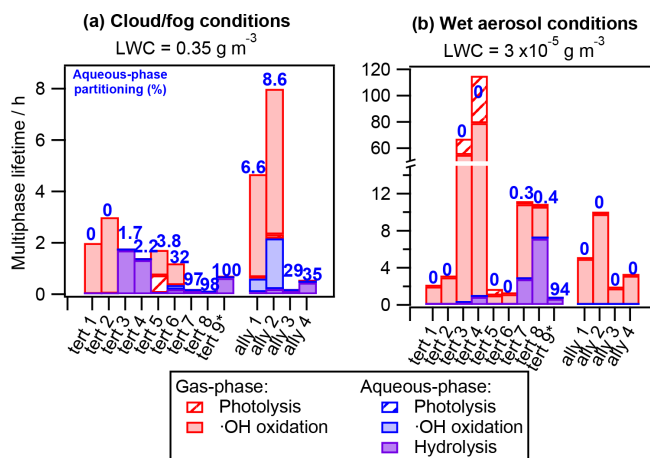


Figure 5. Chemical multiphase lifetimes and relative contribution of each sink of tertiary and allylic RONO₂ under (a) cloud and fog conditions ($LWC = 0.35 \text{ g m}^{-3}$) and (b) wet aerosol conditions ($LWC = 3 \times 10^{-5} \text{ g m}^{-3}$). The numbers in blue indicate the aqueous-phase molar fraction (in %). The chemical structures, properties, and kinetic-rate constants of each compound are listed in Table S4.

with higher water solubilities, such as RONO₂-bearing carbonyl groups and/or presenting low hyperconjugation, since these molecules tend to present longer hydrolysis lifetimes (Wang et al., 2021). This is of high importance, since many authors tend to assume short atmospheric lifetimes due to fast hydrolysis (within hours) for large fractions of atmospheric RONO₂ (Fisher et al., 2016; Zare et al., 2019; Browne et al., 2013), while the decay of these RONO₂ can actually be mostly controlled by the aqueous-phase $\cdot\text{OH}$ reactivity.

4.3 Overall RONO₂ multiphase lifetimes

Finally, overall multiphase lifetimes of 45 RONO₂ were calculated by including the contribution of dry and wet deposition using Eq. (7). These 45 compounds were classified into (i) non-hydrolyzable small RONO₂, (ii) non-hydrolyzable isoprene and terpene nitrates, and (iii) hydrolyzable RONO₂.

$$\tau_{\text{multiphase}} = \frac{1}{\varphi_{\text{aq}} \cdot k_{\text{hyd}} + \varphi_{\text{aq}} \cdot J_{\text{aq}} + \varphi_{\text{aq}} \cdot k_{\text{OH,aq}} \cdot [\text{OH}]_{\text{aq}} + \varphi_{\text{gas}} \cdot J_{\text{gas}} + \varphi_{\text{gas}} \cdot k_{\text{OH,gas}} \cdot [\text{OH}]_{\text{gas}} + k_{\text{dep}}}, \quad (7)$$

where k_{dep} is the deposition-rate constant (in s^{-1}) that accounts for both dry and wet deposition. The assignment of k_{dep} to each RONO₂ is detailed in Sect. S6.3.

Figure 6 shows the overall lifetimes of all investigated RONO₂ under both cloud and fog conditions (Fig. 6a) and wet aerosol conditions (Fig. 6b). Furthermore, the relative contribution of each sink (deposition, aqueous-phase reactivity, and gas-phase reactivity) is represented.

The results show that all sinks (deposition and aqueous-phase and gas-phase reactivity) significantly contribute to the

RONO₂ atmospheric consumption. However, the contribution of each sink and the overall RONO₂ atmospheric lifetimes depend largely on the RONO₂ chemical structure and the LWC. These parameters can thus highly impact the NO_x atmospheric transport. Hereafter, we discuss the results for each class of RONO₂.

Non-hydrolyzable small RONO₂. Due to their low reactivity, they present the highest lifetimes (between 12 and 97 h). These lifetimes barely vary under both investigated scenarios, since the compounds hardly partition to the aqueous phase in any scenario. The lifetimes are especially larger for alkyl nitrates, since deposition-rate constants are much lower. Under these circumstances, alkyl nitrates are majorly responsible for NO_x flatter distribution due to their long-range atmospheric transport. Furthermore, its sink is mostly controlled by gas-phase chemistry, which is responsible for NO_x recovery.

Non-hydrolyzable isoprene and terpene nitrates. They present shorter lifetimes (between 2 and 15 h) than those of small RONO₂. In general, their atmospheric lifetimes are mostly controlled by chemical sinks although deposition is considerable (38 % and 33 % under cloud and fog and wet aerosol conditions, respectively). Their average lifetimes are slightly longer under cloud and fog conditions (6.1 h vs. 5.4 h under wet aerosol conditions) due to their lower reactivity in the aqueous phase. This increase in the atmospheric lifetime with increasing LWC is especially important for RONO₂ with intermediate to high water solubility ($K_{\text{H}} = 10^5\text{--}10^9 \text{ M atm}^{-1}$) and the presence of conjugated carbonyl groups (the increase is up to 2 times). The less-reactive nature of RONO₂ in the aqueous phase increases the relative contribution of deposition sinks (up to 2 times) under cloud and fog conditions. Therefore, for this kind of compound, an LWC increase would result in lower NO_x recycling efficiencies, since deposition represents a permanent NO_x sink, although RONO₂ are likely transported further. One should also note the importance of aqueous-phase reactivity for terpene nitrates even under wet aerosol conditions. This highlights the importance of understanding the contribution of this reactivity to NO_x formation.

Hydrolyzable RONO₂. Much shorter lifetimes are estimated under cloud and fog conditions (average 1.6 vs. 4.9 h) mostly due to the fast hydrolysis of RONO₂ with high hydrolysis-rate constants (*tert* 1–5 and *ally* 3 and 4). The atmospheric lifetimes of these RONO₂ can be shortened by 2 orders of magnitude. Due to the shortening on their atmospheric lifetimes and the irreversible loss of the nitrate group through hydrolysis, these RONO₂ likely transport much less effectively NO_x at increasing LWC.

5 Conclusions

Photolysis-rate constants and quantum yields were determined in the liquid phase for the first time for isopropyl

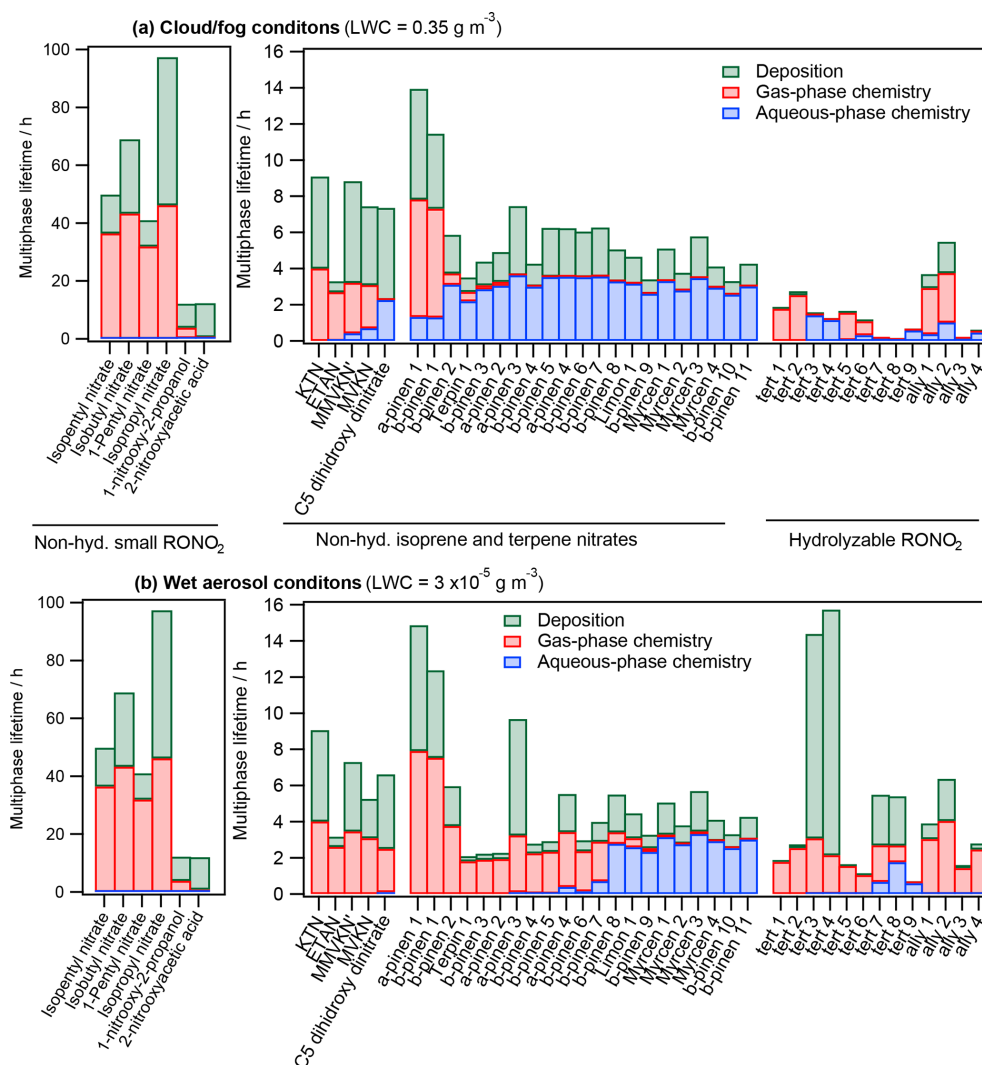


Figure 6. Multiphase atmospheric lifetimes and relative contributions of each sink for 45 atmospherically relevant RONO₂ distributed into (i) non-hydrolyzable small RONO₂ (SN), (ii) non-hydrolyzable isoprene nitrates (IN) and terpene nitrates (TN), and (iii) hydrolyzable RONO₂ (HN) under (a) cloud and fog conditions ($LWC = 0.35 \text{ g m}^{-3}$) and (b) wet aerosol conditions ($LWC = 3 \times 10^{-5} \text{ g m}^{-3}$).

nitrate, isobutyl nitrate, α -nitrooxyacetone, and 1-nitrooxy-2-propanol. Photolysis of these compounds was shown to be hindered in the liquid phase compared to the gas phase. Although they generally presented higher absorption cross-sections when dissolved in the liquid phase, lower quantum yields were observed compared to the gas phase (0.002–0.39 versus ~ 1), probably due to solvent cage effects.

Furthermore, no significant differences were observed in the aqueous-phase photolysis-rate constants between various RONO₂ containing a carbonyl group, a hydroxy group, or neither of them. In contrast, previous studies have shown that the gas-phase photolysis of RONO₂ is greatly enhanced for α - or β -carbonyl nitrates. Our results showed much lower photolysis rates for carbonyl nitrates in the aqueous phase and thus longer photolysis atmospheric lifetimes than in the gas phase. This is of special relevance for these compounds

in the atmosphere, since photolysis is expected to be their major sink.

Considering two different scenarios, (i) cloud and fog conditions ($LWC = 0.35 \text{ g m}^{-3}$) and (ii) wet aerosol conditions ($LWC = 3 \times 10^{-5} \text{ g m}^{-3}$), a complete evaluation of the atmospheric sinks of 45 RONO₂ was performed, including aqueous- and gas-phase $\bullet\text{OH}$ oxidation and photolysis, hydrolysis, and dry and wet deposition. The results highlighted the importance of aqueous-phase $\bullet\text{OH}$ oxidation, a major sink for some RONO₂ even under low LWC, whereas aqueous-phase photolysis remained of negligible importance. The results also emphasized the influence of the RONO₂ chemical structure on RONO₂ atmospheric fate and thus their ability to transport NO_x. The chemical structure of each RONO₂ can influence the kinetics of its multiphase re-

activity and its partitioning between the aqueous and the gas phase.

Small RONO_2 such as alkyl nitrates barely partition into the aqueous phase (even under high LWC conditions). Furthermore, they present low gas-phase reactivity due to their low number of reactive sites and absence of highly reactive groups. Hence, these RONO_2 present the longest lifetimes and thus are responsible for the NO_x flatter distribution.

The atmospheric fate of polyfunctional RONO_2 such as isoprene and terpene nitrates highly depends on their chemical structure. Some tertiary and allylic RONO_2 present very high hydrolysis-rate constants ($k_{\text{hyd}} > 5 \times 10^{-4} \text{ s}^{-1}$). For these compounds, hydrolysis is the only sink even when they mildly partition to the aqueous phase ($\varphi_{\text{aq}} > 0.4 \%$). Their atmospheric lifetimes can decrease drastically (up to 2 orders of magnitude) with increasing LWC, and under these conditions, their processing represents a net sink of NO_x . Out of these results, it is evident that more research should be done to clearly elucidate the influence of the RONO_2 chemical structure on the hydrolysis-rate constant.

The fate of polyfunctional RONO_2 with low or negligible hydrolysis ($k_{\text{hyd}} < 1 \times 10^{-4} \text{ s}^{-1}$) is mainly controlled by their atmospheric partitioning. For molecules with low water solubility ($K_{\text{H}} < 10^4 \text{ M atm}^{-1}$), their fate is mainly controlled by their gas-phase reactivity and dry deposition. Their atmospheric lifetimes are lower than those of alkyl RONO_2 (ranging from 2 to 15 h) and are impacted by the presence of conjugated carbonyl groups (fast photolysis), aldehyde groups, and double bonds (fast $\bullet\text{OH}$ oxidation). They may thus recycle NO_x . RONO_2 with intermediate water solubilities ($K_{\text{H}} = 10^5\text{--}10^9 \text{ M atm}^{-1}$) show more complex processing, their atmospheric fate and lifetimes highly depend on the LWC. At high LWC, their sink is mainly controlled by aqueous-phase $\bullet\text{OH}$ oxidation and dry and wet deposition, while at low LWC, gas-phase $\bullet\text{OH}$ oxidation and photolysis are the main sinks. Due to the decrease of the RONO_2 reactivity in condensed phases, their atmospheric lifetimes increase with increasing LWC (up to 2 times greater). Furthermore, the overall importance of non-chemical sinks (deposition) increases with higher LWC. The ability of RONO_2 aqueous-phase $\bullet\text{OH}$ oxidation to recycle NO_x must be investigated to properly predict the impact of their fate, especially since they represent an important fraction of the atmospherically relevant RONO_2 . Finally, RONO_2 with very high water solubility ($K_{\text{H}} \geq 10^{10} \text{ M atm}^{-1}$) partitions to the aqueous phase even under very low LWC, and thus their fate is mainly controlled by aqueous-phase $\bullet\text{OH}$ oxidation and dry and wet deposition.

Data availability. All data related to this article are available at <https://doi.org/10.7910/DVN/O7HKJQ> (González-Sánchez, 2023).

Supplement. The supplement related to this article is available online at: <https://doi.org/10.5194/acp-23-5851-2023-supplement>.

Author contributions. JMGS performed all kinetic experiments, treated all data, and built the atmospheric implication discussion. NB provided the UV-VIS data for RONO_2 . JMGS and SR developed the UHPLC-UV method for RONO_2 . JMGS and JLC performed the organic synthesis of RONO_2 . AM and JLC led the work. JMGS, AM, and JW wrote the article with inputs from all co-authors.

Competing interests. The contact author has declared that none of the authors has any competing interests.

Disclaimer. Publisher's note: Copernicus Publications remains neutral with regard to jurisdictional claims in published maps and institutional affiliations.

Acknowledgements. The authors thank Camille Mouchel-Vallon for his help using the GECKO-A modeling tool.

Financial support. This project has received funding from the European Union's Horizon 2020 research and innovation program under the Marie Skłodowska-Curie (grant no. 713750). It has been carried out with the financial support of the Regional Council of Provence-Alpes-Côte d'Azur and with the financial support of the A*MIDEX (grant no. ANR-11-IDEX-0001-02), funded by the Investissements d'Avenir project funded by the French Government and managed by the French National Research Agency (ANR). This study also received funding from the French CNRS-LEFE-CHAT (Programme National-Les Enveloppes Fluides et l'Environnement-Chimie Atmosphérique – Project “MULTINITRATES”). The authors also acknowledge support from the French National Research Agency (ANR-PRCI) through the projects PARAMOUNT (ANR18-CE92-0038-02), ORACLE (ANR-20-CE93-0008-01_ACT), and AEROFOG (ANR-22-CE92-0051).

Review statement. This paper was edited by Anne Perring and reviewed by two anonymous referees.

References

- Atkinson, R. and Aschmann, S. M.: Rate constants for the reactions of the OH radical with the propyl and butyl nitrates and 1-nitrobutane at $298 \pm 2 \text{ K}$, *Int. J. Chem. Kinet.*, 21, 1123–1129, <https://doi.org/10.1002/kin.550211205>, 1989.
- Barnes, I., Becker, K. H., and Zhu, T.: Near UV absorption spectra and photolysis products of difunctional organic nitrates: Possible importance as NO_x reservoirs, *J. Atmos. Chem.*, 17, 353–373, <https://doi.org/10.1007/BF00696854>, 1993.

- Bedjanian, Y., Morin, J., and Romanias, M. N.: Reactions of OH radicals with 2-methyl-1-butyl, neopentyl and 1-hexyl nitrates. Structure-activity relationship for gas-phase reactions of OH with alkyl nitrates: An update, *Atmos. Environ.*, 180, 167–172, <https://doi.org/10.1016/j.atmosenv.2018.03.002>, 2018.
- Bianco, A., Passananti, M., Brigante, M., and Mailhot, G.: Photochemistry of the cloud aqueous phase: A review, *Molecules*, 25, 423, <https://doi.org/10.3390/molecules25020423>, 2020.
- Browne, E. C., Min, K.-E., Wooldridge, P. J., Apel, E., Blake, D. R., Brune, W. H., Cantrell, C. A., Cubison, M. J., Diskin, G. S., Jimenez, J. L., Weinheimer, A. J., Wennberg, P. O., Wisthaler, A., and Cohen, R. C.: Observations of total RONO_2 over the boreal forest: NO_x sinks and HNO_3 sources, *Atmos. Chem. Phys.*, 13, 4543–4562, <https://doi.org/10.5194/acp-13-4543-2013>, 2013.
- Carbajo, P. G. and Orr-Ewing, A. J.: NO_2 quantum yields from ultraviolet photodissociation of methyl and isopropyl nitrate, *Phys. Chem. Chem. Phys.*, 12, 6084–6091, <https://doi.org/10.1039/c001425g>, 2010.
- Clemetshaw, K. C., Williams, J., Rattigan, O. v., Shallcross, D. E., Law, K. S., and Anthony Cox, R.: Gas-phase ultraviolet absorption cross-sections and atmospheric lifetimes of several C_2 – C_5 alkyl nitrates, *J. Photochem. Photobiol. A*, 102, 117–126, [https://doi.org/10.1016/S1010-6030\(96\)04458-9](https://doi.org/10.1016/S1010-6030(96)04458-9), 1997.
- Darer, A. I., Cole-Filipiak, N. C., O'Connor, A. E., and Elrod, M. J.: Formation and stability of atmospherically relevant isoprene-derived organosulfates and organonitrates, *Environ. Sci. Technol.*, 45, 1895–1902, <https://doi.org/10.1021/es103797z>, 2011.
- Fisher, J. A., Jacob, D. J., Travis, K. R., Kim, P. S., Marais, E. A., Miller, C. C., Yu, K., Zhu, L., Yantosca, R. M., Sulprizio, M. P., Mao, J., Wennberg, P. O., Crounse, J. D., Teng, A. P., Nguyen, T. B., Clair, J. M. S., Cohen, R. C., Romer, P., Nault, B. A., Wooldridge, P. J., Jimenez, J. L., Campuzano-Jost, P., Day, D. A., Hu, W., Shepson, P. B., Xiong, F., Blake, D. R., Goldstein, A. H., Misztal, P. K., Hanisco, T. F., Wolfe, G. M., Ryerson, T. B., Wisthaler, A., and Mikoviny, T.: Organic nitrate chemistry and its implications for nitrogen budgets in an isoprene- and monoterpene-rich atmosphere: Constraints from aircraft (SEAC4RS) and ground-based (SOAS) observations in the Southeast US, *Atmos. Chem. Phys.*, 16, 5969–5991, <https://doi.org/10.5194/acp-16-5969-2016>, 2016.
- González-Sánchez, J. M.: Replication Data for: On the importance of multiphase photolysis of organic nitrates on their global atmospheric removal, Harvard Dataverse [data set], <https://doi.org/10.7910/DVN/O7HKJQ>, 2023.
- González-Sánchez, J. M., Brun, N., Wu, J., Morin, J., Temime-Roussel, B., Ravier, S., Mouchel-Vallon, C., Clément, J.-L., and Monod, A.: On the importance of atmospheric loss of organic nitrates by aqueous-phase $\bullet\text{OH}$ oxidation, *Atmos. Chem. Phys.*, 21, 4915–4937, <https://doi.org/10.5194/acp-21-4915-2021>, 2021.
- Herrmann, H.: On the photolysis of simple anions and neutral molecules as sources of O^-/OH , SO_x^- and Cl in aqueous solution, *Phys. Chem. Chem. Phys.*, 9, 3935–3964, <https://doi.org/10.1039/b618565g>, 2007.
- Hu, K. S., Darer, A. I., and Elrod, M. J.: Thermodynamics and kinetics of the hydrolysis of atmospherically relevant organonitrates and organosulfates, *Atmos. Chem. Phys.*, 11, 8307–8320, <https://doi.org/10.5194/acp-11-8307-2011>, 2011.
- Jacobs, M. I., Burke, W. J., and Elrod, M. J.: Kinetics of the reactions of isoprene-derived hydroxynitrates: Gas phase epoxide formation and solution phase hydrolysis, *Atmos. Chem. Phys.*, 14, 8933–8946, <https://doi.org/10.5194/acp-14-8933-2014>, 2014.
- Jenkin, M. E., Valorso, R., Aumont, B., Rickard, A. R., and Wallington, T. J.: Estimation of rate coefficients and branching ratios for gas-phase reactions of OH with aliphatic organic compounds for use in automated mechanism construction, *Atmos. Chem. Phys.*, 18, 9297–9328, <https://doi.org/10.5194/acp-18-9297-2018>, 2018.
- Kiendler-Scharr, A., Mensah, A. A., Friese, E., Topping, D., Nemitz, E., Prevot, A. S. H., Äijälä, M., Allan, J., Canonaco, F., Canagaratna, M., Carbone, S., Crippa, M., Dall'Osto, M., Day, D. A., de Carlo, P., di Marco, C. F., Elbern, H., Eriksson, A., Frenay, E., Hao, L., Herrmann, H., Hildebrandt, L., Hillamo, R., Jimenez, J. L., Laaksonen, A., McFiggans, G., Mohr, C., O'Dowd, C., Otjes, R., Ovadnevaite, J., Pandis, S. N., Poulain, L., Schlag, P., Sellegri, K., Swietlicki, E., Tiitta, P., Vermeulen, A., Wahner, A., Worsnop, D., and Wu, H. C.: Ubiquity of organic nitrates from nighttime chemistry in the European submicron aerosol, *Geophys. Res. Lett.*, 43, 7735–7744, <https://doi.org/10.1002/2016GL069239>, 2016.
- Madronich, S.: Photodissociation in the atmosphere: I. Actinic flux and the effects of ground reflections and clouds, *J. Geophys. Res.*, 92, 9740–9752, <https://doi.org/10.1029/jd092id08p09740>, 1987.
- Madronich, S. and Flocke, S.: The Role of Solar Radiation in Atmospheric Chemistry, Springer, Berlin, Heidelberg, 1–26, https://doi.org/10.1007/978-3-540-69044-3_1, 1999.
- Morin, J., Bedjanian, Y., and Romanias, M. N.: Kinetics and Products of the Reactions of Ethyl and *n*-Propyl Nitrates with OH Radicals, *Int. J. Chem. Kinet.*, 48, 822–829, <https://doi.org/10.1002/kin.21037>, 2016.
- Müller, J. F., Peeters, J., and Stavrou, T.: Fast photolysis of carbonyl nitrates from isoprene, *Atmos. Chem. Phys.*, 14, 2497–2508, <https://doi.org/10.5194/acp-14-2497-2014>, 2014.
- Ng, N. L., Brown, S. S., Archibald, A. T., Atlas, E., Cohen, R. C., Crowley, J. N., Day, D. A., Donahue, N. M., Fry, J. L., Fuchs, H., Griffin, R. J., Guzman, M. I., Herrmann, H., Hodzic, A., Iinuma, Y., Kiendler-Scharr, A., Lee, B. H., Luecken, D. J., Mao, J., McLaren, R., Mutzel, A., Osthoff, H. D., Ouyang, B., Picquet-Varraut, B., Platt, U., Pye, H. O. T., Rudich, Y., Schwantes, R. H., Shiraiwa, M., Stutz, J., Thornton, J. A., Tilgner, A., Williams, B. J., and Zaveri, R. A.: Nitrate radicals and biogenic volatile organic compounds: Oxidation, mechanisms, and organic aerosol, *Atmos. Chem. Phys.*, 17, 2103–2162, <https://doi.org/10.5194/acp-17-2103-2017>, 2017.
- Nguyen, T. B., Crounse, J. D., Teng, A. P., Clair, J. M. S., Paulot, F., Wolfe, G. M., and Wennberg, P. O.: Rapid deposition of oxidized biogenic compounds to a temperate forest, *P. Natl. Acad. Sci. USA*, 112, E392–E401, <https://doi.org/10.1073/pnas.1418702112>, 2015.
- Nissenson, P., Dabdub, D., Das, R., Maurino, V., Minero, C., and Vione, D.: Evidence of the water-cage effect on the photolysis of NO_3^- and FeOH_2^+ , Implications of this effect and of H_2O_2 surface accumulation on photochemistry at the air-water interface of atmospheric droplets, *Atmos. Environ.*, 44, 4859–4866, <https://doi.org/10.1016/j.atmosenv.2010.08.035>, 2010.
- Perring, A. E., Pusede, S. E., and Cohen, R. C.: An observational perspective on the atmospheric impacts of alkyl and multifunc-

- tional nitrates on ozone and secondary organic aerosol, *Chem. Rev.*, 113, 5848–5870, <https://doi.org/10.1021/cr300520x>, 2013.
- Picquet-Varraut, B., Suarez-Bertoa, R., Duncianu, M., Cazaunau, M., Pangui, E., David, M., and Doussin, J. F.: Photolysis and oxidation by OH radicals of two carbonyl nitrates: 4-nitrooxy-2-butanone and 5-nitrooxy-2-pentanone, *Atmos. Chem. Phys.*, 20, 487–498, <https://doi.org/10.5194/acp-20-487-2020>, 2020.
- Renard, P., Siekmann, F., Gandolfo, A., Socorro, J., Salque, G., Ravier, S., Quivet, E., Clément, J.-L. L., Traikia, M., Delort, A.-M. M., Voisin, D., Vuitton, V., Thissen, R., and Monod, A.: Radical mechanisms of methyl vinyl ketone oligomerization through aqueous phase OH-oxidation: On the paradoxical role of dissolved molecular oxygen, *Atmos. Chem. Phys.*, 13, 6473–6491, <https://doi.org/10.5194/acp-13-6473-2013>, 2013.
- Rindelaub, J. D., McAvey, K. M., and Shepson, P. B.: The photochemical production of organic nitrates from α -pinene and loss via acid-dependent particle phase hydrolysis, *Atmos. Environ.*, 100, 193–201, <https://doi.org/10.1016/j.atmosenv.2014.11.010>, 2015.
- Rindelaub, J. D., Borca, C. H., Hostetler, M. A., Slade, J. H., Lipton, M. A., Slipchenko, L. V., and Shepson, P. B.: The acid-catalyzed hydrolysis of an α -pinene-derived organic nitrate: Kinetics, products, reaction mechanisms, and atmospheric impact, *Atmos. Chem. Phys.*, 16, 15425–15432, <https://doi.org/10.5194/acp-16-15425-2016>, 2016.
- Roberts, J. M. and Fajer, R. W.: UV Absorption Cross Sections of Organic Nitrates of Potential Atmospheric Importance and Estimation of Atmospheric Lifetimes, *Environ. Sci. Technol.*, 23, 945–951, <https://doi.org/10.1021/es00066a003>, 1989.
- Romer, P. S., Wooldridge, P. J., Crounse, J. D., Kim, M. J., Wennberg, P. O., Dibb, J. E., Scheuer, E., Blake, D. R., Meinardi, S., Brosius, A. L., Thames, A. B., Miller, D. O., Brune, W. H., Hall, S. R., Ryerson, T. B., and Cohen, R. C.: Constraints on Aerosol Nitrate Photolysis as a Potential Source of HONO and NO_x, *Environ. Sci. Technol.*, 52, 13738–13746, <https://doi.org/10.1021/acs.est.8b03861>, 2018.
- Romer Present, P. S., Zare, A., and Cohen, R. C.: The changing role of organic nitrates in the removal and transport of NO_x, *Atmos. Chem. Phys.*, 20, 267–279, <https://doi.org/10.5194/acp-20-267-2020>, 2020.
- Romonosky, D. E., Nguyen, L. Q., Shemesh, D., Nguyen, T. B., Epstein, S. A., Martin, D. B. C., Vanderwal, C. D., Gerber, R. B., and Nizkorodov, S. A.: Absorption spectra and aqueous photochemistry of β -hydroxyalkyl nitrates of atmospheric interest, *Mol. Phys.*, 113, 2179–2190, <https://doi.org/10.1080/00268976.2015.1017020>, 2015.
- Shen, H., Zhao, D., Pullinen, I., Kang, S., Vereecken, L., Fuchs, H., Acir, I. H., Tillmann, R., Rohrer, F., Wildt, J., Kiendler-Scharr, A., Wahner, A., and Mentel, T. F.: Highly Oxygenated Organic Nitrates Formed from NO₃ Radical-Initiated Oxidation of β -Pinene, *Environ. Sci. Technol.*, 55, 15658–15671, <https://doi.org/10.1021/acs.est.1c03978>, 2021.
- Shepson, P. B.: Organic nitrates, Blackwell Publishing Ltd., Oxford, UK, 58–63, <https://doi.org/10.1358/dnp.1999.12.1.863615>, 1999.
- Suarez-Bertoa, R., Picquet-Varraut, B., Tamas, W., Pangui, E., and Doussin, J. F.: Atmospheric fate of a series of carbonyl nitrates: Photolysis frequencies and OH-oxidation rate constants, *Environ. Sci. Technol.*, 46, 12502–12509, <https://doi.org/10.1021/es302613x>, 2012.
- Svoboda, O., Kubelová, L., and Slaviček, P.: Enabling forbidden processes: Quantum and solvation enhancement of nitrate anion UV absorption, *J. Phys. Chem. A*, 117, 12868–12877, <https://doi.org/10.1021/jp4098777>, 2013.
- Takeuchi, M. and Ng, N. L.: Chemical composition and hydrolysis of organic nitrate aerosol formed from hydroxyl and nitrate radical oxidation of α -pinene and β -pinene, *Atmos. Chem. Phys.*, 19, 12749–12766, <https://doi.org/10.5194/acp-19-12749-2019>, 2019.
- Talukdar, R. K., Herndon, S. C., Burkholder, J. B., Roberts, J. M., and Ravishankara, A. R.: Atmospheric fate of several alkyl nitrates: Part 1. Rate coefficients of the reactions of alkyl nitrates with isotopically labelled hydroxyl radicals, *J. Chem. Soc. Faraday T.*, 93, 2787–2796, <https://doi.org/10.1039/a701780d>, 1997a.
- Talukdar, R. K., Burkholder, J. B., Hunter, M., Gilles, M. K., Roberts, J. M., and Ravishankara, A. R.: Atmospheric fate of several alkyl nitrates: Part 2. UV absorption cross-sections and photodissociation quantum yields, *J. Chem. Soc. Faraday T.*, 93, 2797–2805, <https://doi.org/10.1039/a701781b>, 1997b.
- Tilgner, A., Bräuer, P., Wolke, R., and Herrmann, H.: Modelling multiphase chemistry in deliquescent aerosols and clouds using CAPRAM3.0i, *J. Atmos. Chem.*, 70, 221–256, <https://doi.org/10.1007/s10874-013-9267-4>, 2013.
- Wang, Y., Piletic, I. R., Takeuchi, M., Xu, T., France, S., and Ng, N. L.: Synthesis and Hydrolysis of Atmospherically Relevant Monoterpene-Derived Organic Nitrates, *Environ. Sci. Technol.*, 55, 14595–14606, <https://doi.org/10.1021/acs.est.1c05310>, 2021.
- Wängberg, I., Barnes, I., and Becker, K. H.: Atmospheric chemistry of bifunctional cycloalkyl nitrates, *Chem. Phys. Lett.*, 261, 138–144, [https://doi.org/10.1016/0009-2614\(96\)00857-3](https://doi.org/10.1016/0009-2614(96)00857-3), 1996.
- Warneck, P. and Wurzinger, C.: Product quantum yields for the 305-nm photodecomposition of nitrate in aqueous solution, *J. Phys. Chem.*, 92, 6278–6283, 1988.
- Zare, A., Fahey, K. M., Sarwar, G., Cohen, R. C., and Pye, H. O. T.: Vapor-Pressure Pathways Initiate but Hydrolysis Products Dominate the Aerosol Estimated from Organic Nitrates, *ACS Earth Space Chem.*, 3, 1426–1437, <https://doi.org/10.1021/acsearthspacechem.9b00067>, 2019.